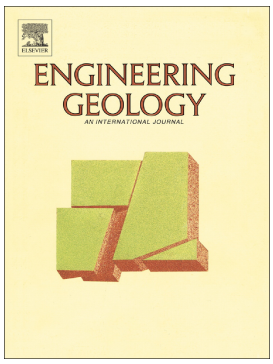

Hydro-geotechnical modelling of subsidence in the Como urban area

Greta Bajni, Tiziana Apuani, Giovanni Pietro Beretta

PII: S0013-7952(18)31568-0
DOI: https://doi.org/10.1016/j.enggeo.2019.105144
Article Number: 105144
Reference: ENGEO 105144

To appear in: *Engineering Geology*

Received date: 11 September 2018
Revised date: 10 May 2019
Accepted date: 15 May 2019

Please cite this article as: G. Bajni, T. Apuani and G.P. Beretta, Hydro-geotechnical modelling of subsidence in the Como urban area, Engineering Geology, https://doi.org/10.1016/j.enggeo.2019.105144

Hydro-geotechnical modelling of subsidence in the Como urban area

Greta Bajni[1,*] greta.bajni@unimi.it*, Tiziana Apuani*[1]*, Giovanni Pietro Beretta*[1]

[1]Department of Earth Sciences “A. Desio”, Università degli Studi di Milano, Via Mangiagalli, 32, 20133, Milan, Italy.

[*]Corresponding author at: Department of Earth Sciences “A. Desio”, University of Milan, Via Mangiagalli, 32, 20133, Milan, Italy.

Abstract

The urban area of Como (Italy) is particularly susceptible to subsidence. The reason is the particular structure of the subsoil, combined with the anthropic modification of the lakeshore lands linked to the historical evolution of the area. Moreover, this phenomenon exposes the lakefront areas to an increasing risk of flooding. The primary purpose of this study was to develop an effective methodology for the assessment of subsidence in urban areas, to be used as a support in groundwater management. The development of a coupled hydrogeological-geotechnical numerical model for the period 2004-2011 allowed recognizing the shoreline results as most susceptible areas to the phenomenon. Model results were critically evaluated through comparison with time series of PSInSAR and high precision levelling data available in the area. The anthropic perturbations of groundwater flow linked to the construction of lake flooding defenses in 2008-2009, enhanced the subsidence phenomenon in a localized area, pointing out the strong inter-dependence of groundwater circulation, lake level oscillations and geotechnical behavior of soils. Thus, the model revealed the most critical zones and geotechnical units, demonstrating to be a potential powerful tool to predict subsidence scenarios (e.g. the future completion of the floods defense works in the shoreline area).

Keywords

Urban subsidence, numerical modelling, hydro-geotechnical coupling, Como.

1. INTRODUCTION

The subsidence phenomenon can occur in a great variety of geomorphological, stratigraphic and structural contexts following both natural processes and anthropic activities, resulting to be one of the major geological risks that characterize urban, coastal and delta areas. Examples of areas

affected by subsidence are the Po Plain in Italy (Antonielli et al., 2016, Carbognin et al., 2004), Mexico (Pacheco-Martínez, 2018), United States' lowlands (Meckel et al., 2006), China's Yangtse Delta (Shi, 2008; Zhang, 2007), Bangkok (Phien-wej, 2006) and Spain (Herrera,2008). Previous researchers outlined that the hydro-mechanical behavior of an aquitard is one of the key points to understand the aquifer-system response to stress variation and to mitigate subsidence (Galloway and Burbey 2011). Aquitards have been frequently investigated through laboratory testing, and on-site stress–strain analysis (Thoang, 2015). Most recently, Gu et al. (2018) combined fiber optic sensing techniques and microstructure analysis of soils to assess subsidence in the Su-Xi-Chang area. Numerical simulation of land subsidence has been increasingly developed in recent years, resulting one of the most powerful tools for predicting the phenomenon and designing the intervention to reduce its impact. Galloway et al. (2003) developed the inverse modeling in MODFLOW (Harbaugh et al., 2000) and added the SUB package to simulate land subsidence and inelastic storage coefficient for Antelope Valley, California. As of China great urban areas, Shi et al. (2012) used a multiscale finite element method (MsFEM) to reproduce the phenomenon in the Suzhou province, while Zhu et al. (2015) used Permanent Scatter Interferometry (PSI) to analyze ground deformation in Beijing. Mahmoudpour (2016) used the IBS1 Package to simulate land deformations in the Teheran Plain in Iran.

The urban historical area of Como (Italy) – also called Convalle – is particularly susceptible to subsidence, because of the particular structure of the subsoil, combined with the anthropic restructuring of the lakeshore lands linked to the historical evolution of the area. Moreover, this phenomenon exposes the lakefront areas to an increasing flood risk with possible damage to buildings, cultural heritage and infrastructures. Since the 1970s, the Municipality has managed the problem, through the establishment of a dedicated commission of specialists – the "*Commissione per lo Studio dei fenomeni di Subsidenza"* in 1974 - and through collaborations with Universities and research institutions. The aim of these studies was to obtain a better understanding of the architecture of the subsoil in a risk management perspective (Apuani et al, 2000, Comerci et al.,2007; Ferrario et al., 2015)..

Most studies concerning subsidence issues regard groundwater withdrawal or oil/gas exploitation; conversely Como's subsoil shows a natural subsidence trend due to the historical management of urbanized lake shoreline. However, the issue was never addressed from a modelling and forecasting perspective and an effective procedure to practically face and predict subsidence phenomenon linked to Como lake levels fluctuations, had not yet been reached. The final objective of the present work is to create a tool able to simulate future risk scenarios in order to promote a conscious management of groundwater and shoreline development in the Como urban area.

The procedural scheme followed in this work includes:

i) The creation and management of a comprehensive database collecting both geotechnical and hydrogeological representative properties and monitoring data;

ii) The definition of the 2D and 3D geotechnical and hydrogeological conceptual models, by means of geostatistical procedures;

iii) The set up of a coupled hydrogeological - geotechnical numerical model to recognize the most critical zones and scenarios of subsidence, due to both natural and anthropic groundwater perturbations.

2. DESCRIPTION OF THE STUDY AREA: GEOLOGICAL, GEOMORPHOLOGICAL AND ENVIRONMENTAL EVOLUTION

Several authors have been described the regional geological setting and the Quaternary evolution of the area in the recent past (Comerci et al. 2004, 2007, Michetti et al. 2013). The town of Como is located in the Southern Alps (Fig. 1a) at the end of the western, hydrologically closed, branch of the lake of Como and stands on a deep sedimentary basin SSE-NNW oriented (> 170 m thick), laterally bordered by rocky slopes. In particular, the East side of the basin is characterized by a thick sequence of Jurassic limestone (*Calcare di Moltrasio*), whereas the West is occupied by a series of Oligo-Miocenic conglomerates (*Gonfolite Lombarda Group*).

The current configuration of the Como plain is linked to the last phases of glacial expansion (LGM) dated in the Alps 21-19 kyr BP and to the final retreat of the Lariano glacier (Ivy-Ochs et al., 2009). During this phase, the deposition of coarse sediments, clays and inorganic silts with dropstones,

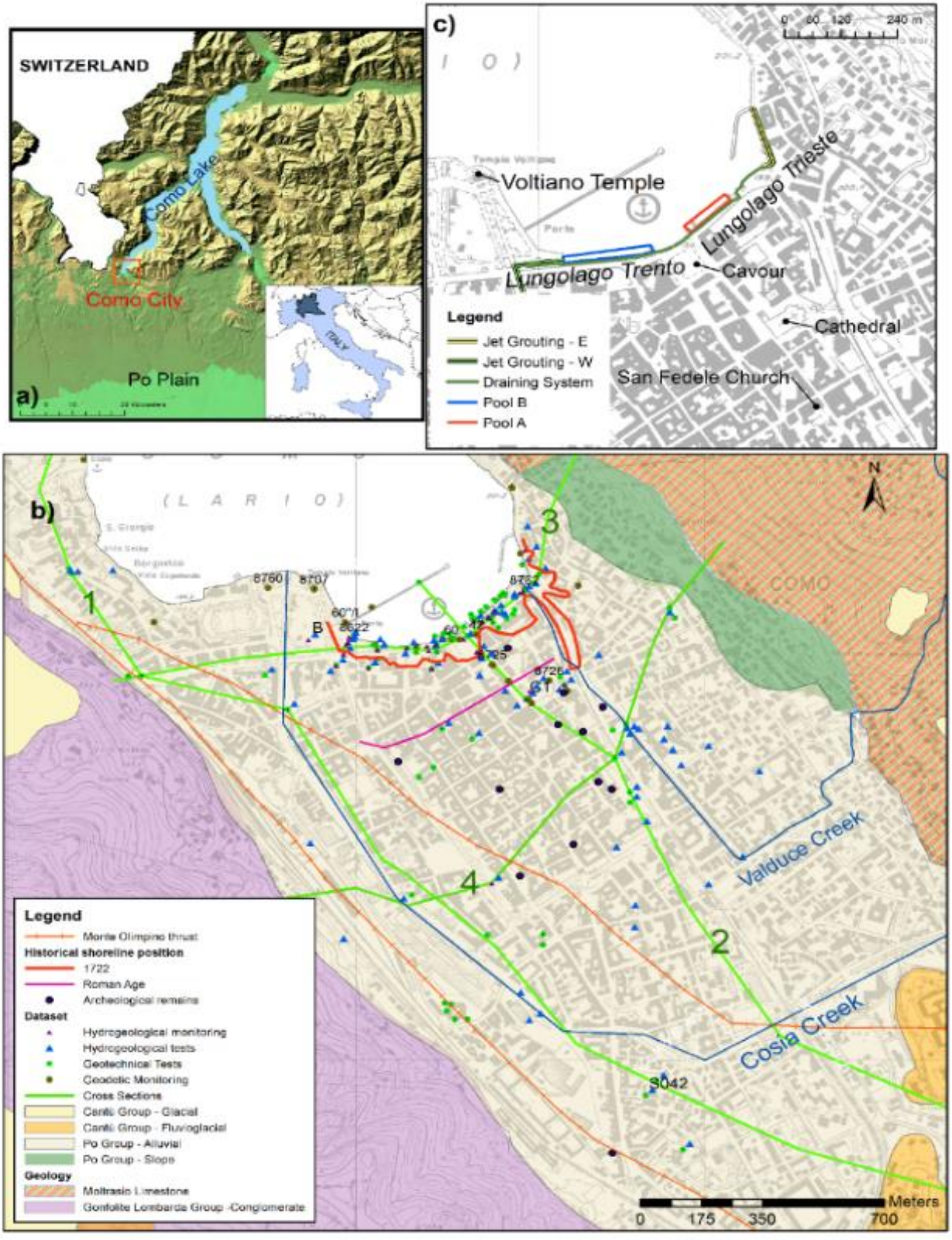

Fig. 1 a) Location of Como city (Italy). b) Geological setting, Shoreline historical reconstruction (Roman Age and 1722, modified from Ferrario, 2015) and dataset point location. Labeled data refers to points used in the numerical model calibration phase. c) Setting for flooding defense works.

indicative of the presence of a wide and deep glacio-lacustrine basin in a cold and arid climate, occurred. With the beginning of a warmer and more humid period, organic sediments began to settle in the lake, in a shallow marsh-lacustrine environment (Ferrario et al, 2015). During this phase, the contribution of coarse sediments was limited, as the local drainage consisted of very small tributaries; only within the marginal zones of the basin, near the reliefs, coarse slope and flood deposits contributed to the filling of the basin (Comerci et al., 2007).

During the Late Holocene, the Cosia creek drainage inversion induced a rapid progradation of the alluvial plain within the marsh basin, with the consequent deposition of gravelly-sandy deposits. The actual coastline and the consequent urbanization are the results of the historical evolution of the city, involved in several episodes of expansion since the Roman Age, including land reclamation of the marshy areas, in addition to the artificial deviation of the Cosia stream. Thanks to the available archaeological and stratigraphic reconstructions (Ferrario et al., 2015), further validated in the through historical cartography examination, coastline advancement (up to 200 m) phases were reconstructed (Fig. 1b).

This progradation process was achieved by the artificial filling of large volumes of reworked anthropic materials along the shoreline, which culminated in 1872 by the filling of the depressed areas of the ancient harbor and the relative creation of the actual *Piazza Cavour*, also known to the many international tourists who frequent the city. The reworked anthropic material is mainly concentrated in the portion between the previous Roman Age shoreline position and the actual coastline; out of this zone the anthropic material is most similar to the underlying alluvial sediments.

From top to bottom, the derived general stratigraphy is composed of 1–15 m of heterogeneous anthropic filling material (at its maximum below *Piazza Cavour*), upper sands and gravels down to the depth of 15–24 m, palustrine silts with organic content down to 23–50 m, inorganic lacustrine clays down to 40–60 m and lower sands and gravels down to 170 m (Comerci, 2007).

Due to the absence of any river outlet, the town was (and still is) subject to continuous lake flooding (e.g. ruinous flood occurred in 2002, 2008, 2010 and 2016); despite the administration's

efforts to mitigate the problem over the years, flooding is still a recurrent situation related to heavy rainfall events. The most recent project to mitigate the problem began in 2008 (last updates: Municipality of Como, 2014) and included the construction of fixed and movable bulkheads, detention tanks (Pool A, placed in Lungo Lario Trieste and Pool B located in Lungo Lario Trento) and jet grouting barriers (Fig. 1c). Works still need to be completed (i.e. creation of Pool A).

3. DATASET CREATION

A site-specific organized database was created, within a GIS platform. The database includes: i) stratigraphic, geotechnical and hydrogeological data, resulting both from in situ and laboratory tests (i.e. CPT, CPTU, SPT, Cross Hole, pumping and on-site permeability tests, oedometric, triaxial, uniaxial tests); ii) groundwater levek monitoring data; and iii) ground elevation monitoring data from both high precision benchmarks and remote sensing (PSInSAR technique).

Some empirical and direct correlations were adopted between geotechnical parameters and in situ test results, to homogenize the great amount of data coming from different acquisition methods (Table 1). Analysis focused on soil geotechnical and hydrogeological properties to which subsidence phenomenon is more sensitive, namely bulk densities, oedometric modulus, compressibility coefficient and index, and void ratio, permeability and storage.

Direct and empirical equation	
$\boldsymbol{E = 7.7Nspt + 191}$	D'Apollonia, 1970
$\boldsymbol{E = 2.5Qc}$	Schmertmann, 1978
$\boldsymbol{Med = 10.46Nstp + 38}$	Menzenbach, 1959
$\boldsymbol{Med = \alpha Qc}$	Sanglerat, 1972
$\boldsymbol{Cc = 1.35IP}$	Wood, 1990
$\boldsymbol{Cc = 0.75(e0 - 0.5)}$	Sowers, 1970

Table 1 Direct and empirical equation adopted to uniform the dataset of subsoil geotechnical parameters.
E= Elastic Modulus; M_{ed}= oedometric Modulus; Nstp=Standard penetration test index e_0=void ratio; IP=Plasticity index; C_c= compressibility index; Q_c=Cone Penetration Test tip resistance; ??=Sanglerat experimental parameter. Equation references:

The comparison between lake and groundwater levels reveals a strong groundwater level dependency on the lake, which attenuates with increasing distance from the shoreline. Ground

elevation monitoring data are numerous, heterogeneous in terms of acquisition and temporally discontinuous, and would be deeper analysed in section 4.

4. RECORDS OF LAND SUBSIDENCE IN THE COMO URBAN AREA

4.1. High precision levelling benchmark analysis

The estimation of historical subsidence rates was carried out based on geometric precision leveling data, discontinuously available from early 1900s to 2014. A total of 27 benchmarks are present in the area, with a higher density among the lakefront area and historical center of Como. However, only few benchmarks recorded an almost complete displacement data series. Data from the he most representative monitoring points were plotted as cumulated subsidence (Fig. 2b) and average annual displacement rates (Fig. 2c). Natural subsidence showed maximum values, between 2.5 and 3 $x10^{-3}$ m/year, in the ancient city center in the proximity of the Lake (Comerci et al., 2007). These evidences are coherent with the poor geotechnical properties of the anthropic material, put in place during the last centuries for the harbor filling. After the Second World War, the natural subsidence tendency has been superimposed by an anthropic contribute, mainly attributable to the excessive exploitation of the aquifer (up to 150 l/s) and characterized by a localized maximum subsidence rates from 1 to 2 $x10^{-3}$ m/year (Arca and Beretta 1985).

The dramatic acceleration of ground sinking made it necessary a strong reduction of groundwater exploitation in the historical town to the current 25 l/s. Despite this, the front lake areas still experiment a deformation trend; this not only causes foundations and roads damage, but it is also closely associated to the frequent Como Lake flooding. Defense works designed for a precise flooding height could be ineffective if located in areas subjected to a greater progressive subsidence.

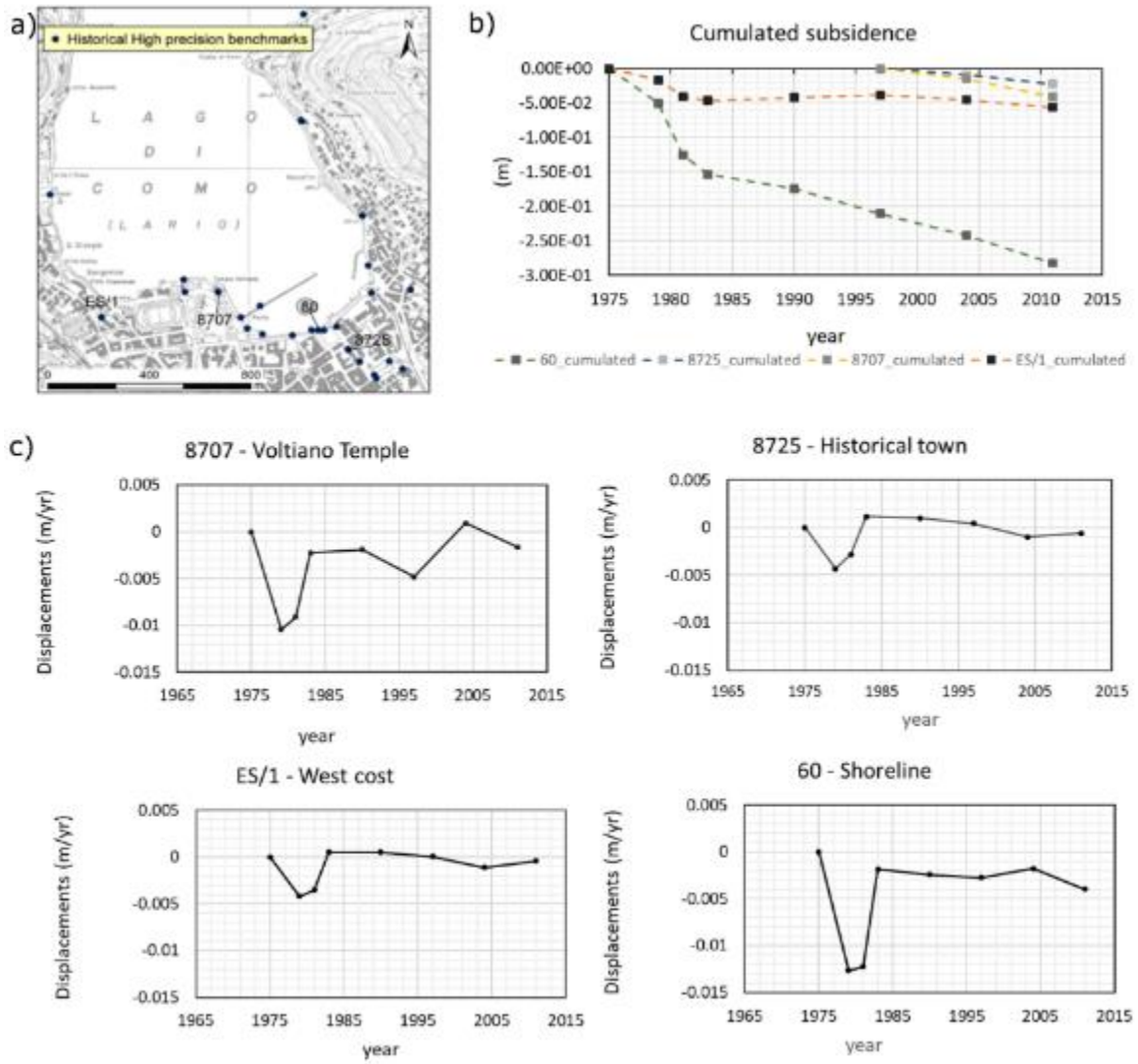

Fig. 2 a) High precision benchmark locations. Analyzed benchmarks are labeled. b) Cumulated subsidence and c) displacement time series of four selected benchmarks.

4.2. Satellite data analysis

For the period 2003-2012, data from RADARSAT-1 sensor were analyzed through the PSInSAR technique by the company TRE Telerilevamento Europa. PSInSAR is a non-invasive surveying technique used to calculate motions of individual ground and structure point-like target over wide-areas (Ferretti et al., 2000; Ciampalini et al. 2014). Each displacement measure provided is one-dimensional and has to be referred along the sensor-target direction (LOS - Line Of Sight), inclined

with respect to the vertical by about 36 ° for Como city. Due to the availability of the only descending acquisition geometry, it is not possible to decompose the motion in the vertical and

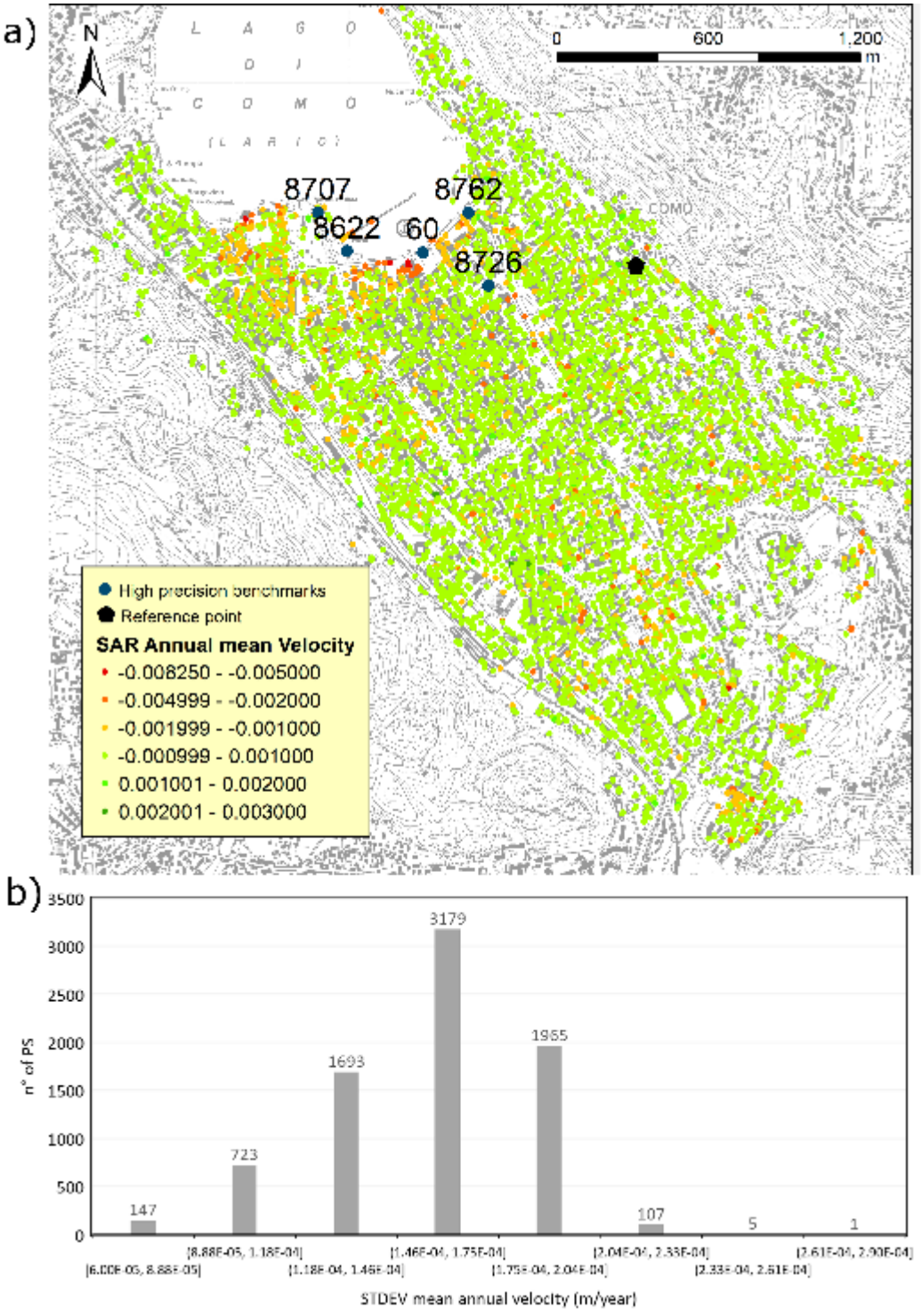

Fig. 3 a) PSInSAR data classified by mean annual displacement velocity (in m/years). Blue labeled dots: high precision points near test sites. Black polygon: Reference point used for PSInSAR technique. b)Frequency histogram of velocity standard deviation.

horizontal components.

Nevertheless, an analysis of PS deformation series has been carried out to obtain the annual mean subsidence velocity for 2004-2011 (Fig. 3a). The stability threshold, which identifies

displacements whose values are not significant, has to be referred and chosen according to the ground deformation velocity standard deviation (STD) of the PS population (Fig. 3b). Standard deviation itself depends on several factors, such as PS distance from the reference point and the radiometric quality of the measure (i.e. phase coherence and atmospheric component). Despite the high accuracy obtained in the study area (i.e. low STD of of 0.09×10^{-3} m/year of stable points near the reference point), PSInSAR maximum accuracy in mean annual velocities below the threshold of 1×10^{-3} m/year is usually considered as not significant due to technique limitations. Therefore, a stability threshold of $\pm 1 \times 10^{-3}$ m/year was selected.

PS response showed a local significance, with different annual displacement rates even between neighbouring points. This is probably attributable to local perturbations (e.g. construction sites, building restorations), which are very frequent in such urban context, where a lot of historical buildings and cultural assets are present. Beyond these limitations, PS time series covering five important urban sites (Lungolago Trento and Trieste, Piazza Cavour, Tempio Voltiano and Duomo Cathedral areas) were deeper analyzed at a larger scale for the period 2004-2011 (Fig. 3).

For each site of interest, some representative complete PS displacement time series (7-8 measurements per year) are plotted in Fig. 4 (dashed lines) together with the average annual displacement series calculated for five PS chosen with a distance among them <10 m (colored lines). The cumulated subsidence since 2004, recorded by the high precision levelling points closer to each analyzed site (locations in Fig. 3) is added (red dots in Fig. 4).

The *Lungolago Trieste* (Fig. 4a) time series reveals a seasonal oscillation linked to lake level variations (Fig. 4b). During the first and last months of each year a negative deformation (subsidence, maximum effective stress and minimum pore pressure) is evident and coherent with low lake levels; during spring and summer months, due to Lake level rise linked probably to snow fusion, a deformation recovery trend (minimum effective stress and maximum pore pressure) could be identified. The medium annual trends of *Lungolago Trieste* area reveal an almost constant slight subsidence rate of the order of 1.5×10^{-3} m/year. The five PS displacement series have quite homogeneous trends, except for the periods between 2004-2005 and 2010-2011, where opposite displacements are recorded, further highlighting PS response to localized perturbations.

Voltiano Temple site (Fig. 4c), close to the shoreline, records a displacement seasonality (dashed lines) similar to the one highlighted previously for Lungolago Trieste. Despite this, the five mean annual displacement trends show a strong discrepancy (especially during 2004-2005 and 2009-2011) reasonably due to the fact that some PS are located on the temple building (e.g. PS 172) and others outside, thus recording foundations differential settlements.

Piazza Cavour (Fig. 4d) has recorded a general and coherent subsidence trend, with some localized inversions of ground movements in correspondence with individual structures and buildings (e.g.. PS001OV). PS located in the eastern part of Piazza Cavour (PS 257 and 0026E) does not show any particular subsidence increment; while those situated in the western flank of the square (PS 257 and 0026E) show an acceleration with negative displacement during 2008-2009 concomitant with the beginning of the construction of the flood defense system.

The same acceleration trend is even more evident in the *Lungolago Trento* area (Fig. 4e), site of the defense works. From 2008 an acceleration in the deformation trend led to a cumulated subsidence of $4x10^{-3}$ m in 2009 and $5x10^{-3}$ m in 2010. Although construction works ended in autumn 2009, a the visible increment of subsidence recorded in 2010 was probably caused by the delayed reaction of the cohesive soils. After 2010, the subsidence rate restores to the one prior to the construction works. It should be note that the horizontal component of the motion along the N-S direction is not detectable by the SAR systems because of the satellite acquisition geometry (parallel orbit to the meridians). Considering that the construction work site is mainly oriented E-O, the displacement data recorded by the satellite may be underestimated with respect to the real displacement vector module. Indeed PS considered in Fig. 4e resulted to have the highest standard deviation in the area; moreover, those points are located near the construction site and not above it, where the pumping effect is expected to be maximum.

Duomo cathedral site shows a general low subsidence rate, except for a more pronounced displacement during 2004-2005. This behavior, in addition to its distance from the shoreline, suggests a limited influence of the lake level changes on the subsidence phenomenon. This is confirmed by the non-dependence of the displacement time series (dashed line) on seasonal Lake

level variations, differently to what recorded along the shoreline. Opposite displacement trends, between points on and outside Duomo building are recorded (Fig. 4f).

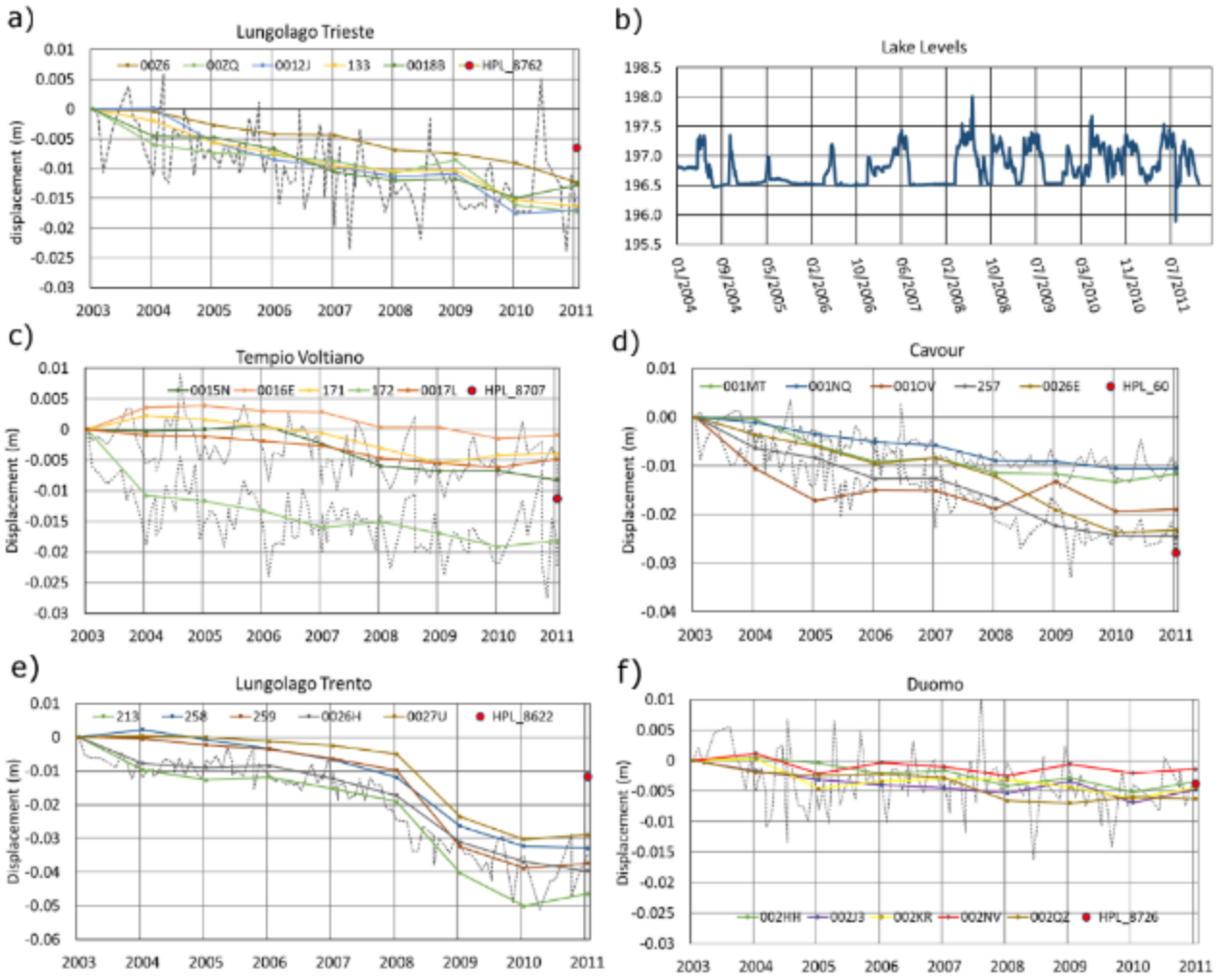

Fig. 4 PS displacement time series (dotted lines), PS medium annual displacement (coloured lines) and benchmarks cumulated displacement in the period 2004-2011 (Red points) for five urban sites.b)Lake Levels collected along the shoreline.

Satellite data allowed identifying a general and continuous spatial distribution of the studied phenomenon as well as local cause-effect relationships. Nevertheless, the PS analysis results cannot be taken as representative absolute values of ground movements, due to the above mentioned technical limitations. Therefore, displacements recorded by high precision levelling benchmarks were preferred for the calibration phase of the numerical model.

5. HYDRO-GEOTECHNICAL DATA ANALYSIS AND CONCEPTUAL MODEL

The lithostratigraphic heterogeneity of the area, attributable to the variety of transport agents and

depositional environments, affects the geotechnical characteristics of the soils and therefore, with an equally great variability, their behavior under stresses. Moreover, in the early stages, the depositional process was interrupted by successive glacial advances that partially eroded and deformed the oldest sediments; then the fluvial deposition of sedimentary bodies in erosion on the other sediments is also registered. For these reasons, deposits are discontinuous and characterized by marked lateral heteropies.

The stratigraphic, hydrogeological and geotechnical information along each borehole, supported by the surface geological survey, were re-interpreted defining the aquifer system with five homogeneous geotechnical units characterized by uniform behavior in terms of groundwater flow and subsidence susceptibility. Coarser deposits were characterized based on grain-size composition, relative density and resistance to the dynamic penetration tests (SPT). Cohesive sediments, were differenziated based on consistency, pocket penetrometer and Vane test results. Furthermore, the re-interpretation of the static penetrometric tests (CPTU) allowed defining the deformation parameters for the five units in on-site confined conditions. The data obtained with laboratory tests, permitted the quantitative definition of the soil index properties and of mechanical behavior (deformability, compressibility and shear strength). The Cross-Hole tests provided the elastic waves velocity values and the dynamic deformation parameters of the various units. Through the joint analysis of stratigraphic interpretation and the geostatistical interpolator of ordinary kriging, the top and bottom surfaces of the identified geotechnical units were reconstructed

The geotechnical stratigraphy thus identified comprises, proceeding from ground level to the depth of about 180 m:

REWORKED ANTHROPIC MATERIALS (R) - Anthropogenic deposits, reworked materials and soils of historical age. The unit is characterized by an extreme thickness, spatial distribution and hydro-mechanical behavior heterogeneity, adequately differentiated by introducing some sub-units (i.e.R_C – Cavour sub-unit, R_{LF} – Lakefront sub-unit and R_{UC} – Urban coarse sub-unit) during the parametrization phase.

UPPER GRAVELLY SANDS (UGS) -Torrent deposits consisting of gravelly heterometric sand, fine gravel with silty sand, sporadic presence of pebbles, with typical granular behavior.

PALUSTRINE ORGANIC SILT (POS) and INORGANIC CLAYEY SILT (ICS) - Silty sediments with a high organic component, present from a depth of 40 ÷ 50 m, passing inferiorly to clayey glacial-lacustrine deposits. Although the palustrine and glacial-lacustrine deposits could be merged from the stratigraphic and depositional point of view, their compressibility is significantly different, being the upper silty-organic portion more compressible.

LOWER SANDS AND GRAVELS (LSG) - Medium and coarse sands, locally silty. The generally high depth (from about 80-100 m) at which their upper limit is located, together with the difficulties encountered in taking undisturbed samples, strongly limit the geotechnical knowledge on the unit. For this reason, and considering the expected low significance of this unit to the subsidence phenomenon, LGS unit was not included in the numerical model.

Plotting each geotechnical data vs depth (Fig. 5) the wide variability of the parameters at low depth is evident, without a well-defined representative value. This is mainly due to the R unit presence within the first 10 meters of depth. Volume weights (γ) and void index (e) could reach very high values, due to the presence of very coarse material and remains of human artifacts inside the unit. The natural water (W_n) content of the unit R, high and close to the value of the liquid limit is attributable to the portion constituted by recent silt lacustrine deposits; W_n results high even at significant depths in correspondence of POS and ICS units, in accordance with the fine nature of the sediments. Each unit's representative oedometric module (*Med*), fundamental for defining the deformative behavior, derives from a critical analysis of data collected by different sources e.g. oedometric tests, direct relationship with SPT and CPT tests, empirical methods and literature data, on the basis of the soils nature and method reliability.

Regarding the hydrological and hydrogeological conceptual model, the area can be considered of a certain hydrological complexity. In fact, in addition to the morphological articulation of the areas and the fragmentary nature of the basins, there is a multidirectional groundwater circulation: centripetal, towards the lake, in a large part of the territory; centrifugal, but in more directions, in the southern part.

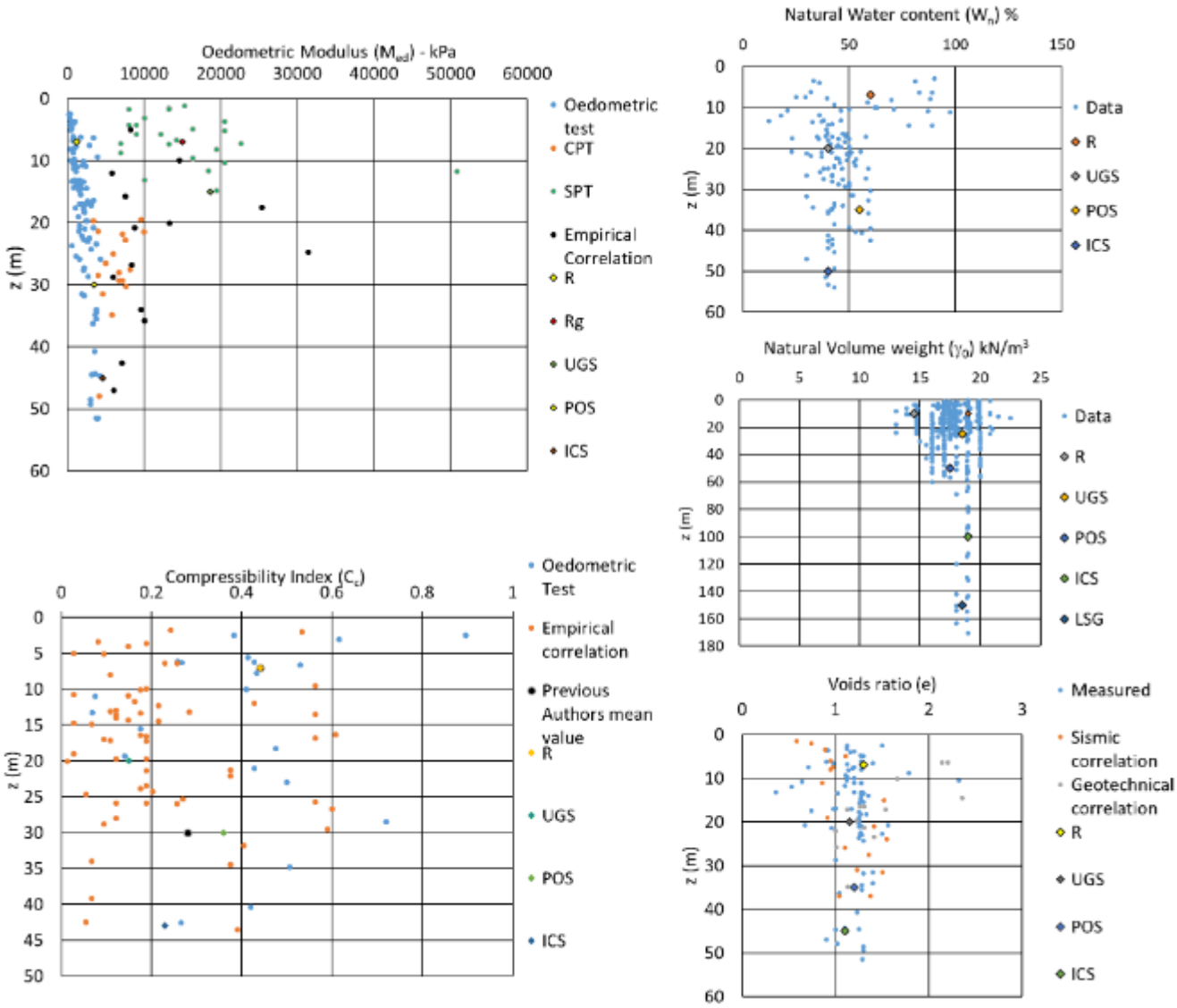

Fig. 5 Geotechnical properties (natural volume weight, natural volumetric content of water, void ratio, compressibility index and the oedometric modulus) versus depth. In γ_0 and W_n graphs the whole data present in the dataset are marked by blue dots.

The re-interpretation of geotechnical units in a hydrogeological key has led to the definition of three hydrogeological units, continuously detectable within the entire urban area. These units are: a surficial unconfined aquifer, locally (especially in the lake front area) semi-confined (R and UGS units), a semipermeable-impermeable aquitard horizon (POS and ICS units) separating the first aquifer from the deep aquifer system, seat of confined circulation (LSG unit).

Fig. 6 shows four sections - two longitudinal and two transversal with respect to the central axis of the study area - extrapolated from the three dimensional stratigraphic-geotechnical model.

Observing the geometry of the subsoil bodies, extreme heterogeneity in the thicknesses of the R unit is once again highlighted, which thicknesses of up to 10-15 m in the eastern and axial area of the Como lakeshore, and then maintain a constant thickness of about 3 m in the rest of the urban area. The underlying unit, UGS, reaches its maximum thickness approximately in the central part of the urban area and then show a strong reduction at the margins, more accentuated to NE, going to close in eterophy with slope and glacial deposits. POS and ICS units follow the geometric trend of the overlying unit: in particular, in the eastern area of the city, the POS unit becomes thinner up to 2 m. Generally, the contacts between the units were observed of an erosive nature, with marked

irregularities of the surface.

6. NUMERICAL MODEL

6.1. Modelling Approach and background theory

Using the previous created database and the subsoil geotechnical reconstruction (conceptual model), a groundwater flow numerical model was created by MODFLOW 2000 (Harbaugh et al. 2000). Land subsidence was afterwards simulated by the MODFLOW modular SUB Package (Hoffmann et al. 2003). The SUB package is based on the theory of one-dimensional (vertical)

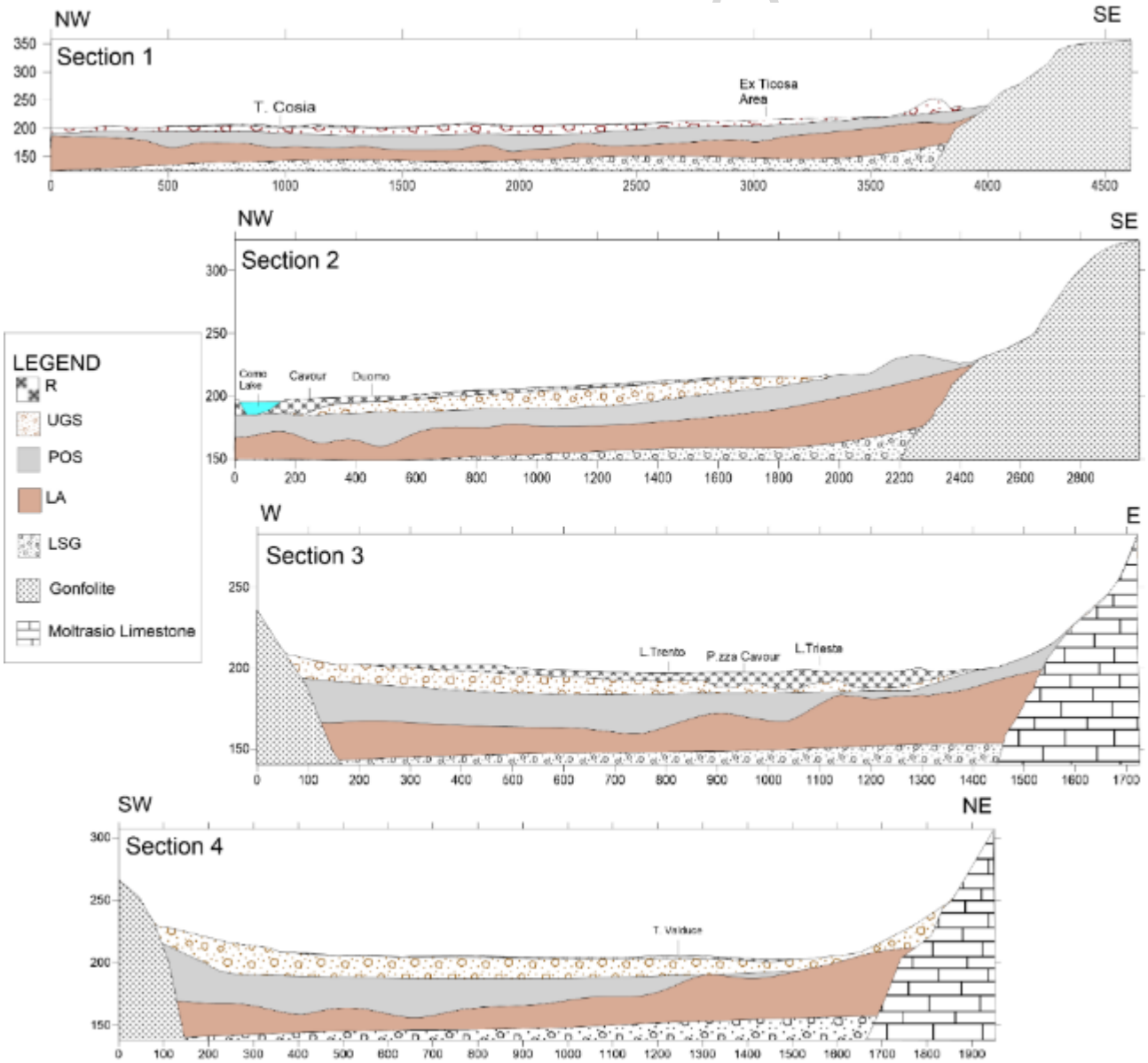

Fig. 6 Simplified cross sections extrapolated from the 3D conceptual model. Location of cross sections is shown in Fig. 1.

consolidation, developed by Terzaghi (1925), which assumes that deformation is vertical and that the total stress does not vary and thus, changes in hydraulic head produces equal but opposite changes in effective stress. The main equation on which the subsidence simulation relies is the flow equation:

$$\frac{\partial}{\partial x}\left(K_{xx}\frac{\partial h}{\partial x}\right)+\frac{\partial}{\partial y}\left(K_{yy}\frac{\partial h}{\partial y}\right)+\frac{\partial}{\partial z}\left(K_{zz}\frac{\partial h}{\partial z}\right)-W=S_s\frac{\partial h}{\partial t} \quad (1)$$

in which K_{jj} (m/s) represents the hydraulic conductivity in each of the three dimension (*x, y, z)*, *h* (m) is the hydraulic load, *W* (m) is the volumetric flow per unit of volume representing sources or withdrawals of water and S_s (m^{-1}) the specific storage of porous media.

To this equation SUB package implements the amount of drained water from interbeds and aquitards during the compaction phase. Soil deformation of aquifers of thickness *b (m)*, caused by level drop (Δh), is described by:

$$\Delta b = S_{sk} b \Delta h \quad (2)$$

where S_{sk} represents the skeletal component of specific storage and is linked to the expansion or compression of the sediment that results from a change in effective stress; therefore it could be expressed in terms of the skeletal compressibility m_v (Hoffman et al., 2003):

$$S_{sk} = \rho_w g m_v$$

Skeletal compressibilities of fine-grained aquitards and coarser-grained aquifers typically differ by several orders of magnitude (Riley, 1969). Skeletal specific storages of the aquitards are defined for two ranges of stress, elastic (S_{ske}) and inelastic (S_{skv}). In the context of aquifer systems, the past maximum stress, or preconsolidation stress, can generally be represented by the previous lowest ground-water level. For stresses lower than the preconsolidation stress – i.e. ground-water level higher than that corresponding to the preconsolidation level – the aquifer system deforms (compresses or expands) elastically, and the deformation is recoverable. For stresses beyond the preconsolidation stress – i.e. ground-water levels lower than that corresponding to the preconsolidation level – the pore structure of susceptible fine-grained sediments in the system may undergo significant rearrangement, resulting in a permanent (inelastic) reduction of pore volume and vertical displacement of the land surface, or land subsidence (Sneed, 2001).

Through the SUB package, it is possible to simulate subsidence of both continuous aquitards and thin interbeds by choosing two different simulation approaches *No-delay interbeds* and *delay interbeds*, respectively. *No-delay interbeds* assumes an almost instantaneous compaction that fits a basin scale simulation, while *Delay interbeds* considers the delay τ (s) in the dissipation of the pressures and therefore the compaction is explicitly simulated. This delay is explicited by Riley equation (1969):

$$\tau = \frac{S_{skv}\left(\frac{b}{2}\right)^2}{K_v} \quad (4)$$

where S_{skv} is aquitard inelastic skeletal specific storage, b is the thickness of the aquitard, and K_v is aquitard vertical hydraulic conductivity. To calculate the delay, the package requires to quantify the number and thickness of each individual interbed present in the aquifer.

6.2. Spatial and temporal discretization and boundary conditions

To simulate the stratigraphic succession of the study area, a three-dimensional grid of 561 x 524 square cells with 5 m per side was created. The aquifer system was vertically discretized by four Layers representing the first four geotechnical units (R, UGS, POS and ICS). The geometry of each layer was imported in the numerical code as interpolated during the geostatistical construction of the conceptual model. The period chosen for the simulation covers eight years from 2004 to 2011, as it is the recent period with the most frequent and continuous data recording. The simulation was performed by nine stress periods: the first corresponds to a steady state simulation, while the other eight (each representing one “annual scenario” from 2004 to 2011) model unsteady conditions.

A *No-FLOW* boundary condition was attributed to all the cells of the model that fell in correspondence with the rocky reliefs that are excluded from the simulation of groundwater flow. The *CHD (Constant Head)* condition was used in simulating the hydraulic head of Como Lake, in the northern part of the model, in accordance with its fundamental role in regulating the basin groundwater levels, especially in the shoreline area. Nevertheless, it was considered appropriate, for the prefixed precision level (i.e. the spatial distribution of annual subsidence), to fix the *CHD* of each simulated year to the relative average annual height of the lake while, for the first steady state stress period the highest mean value of 198 m a.s.l. was assigned. This choice is justified by the

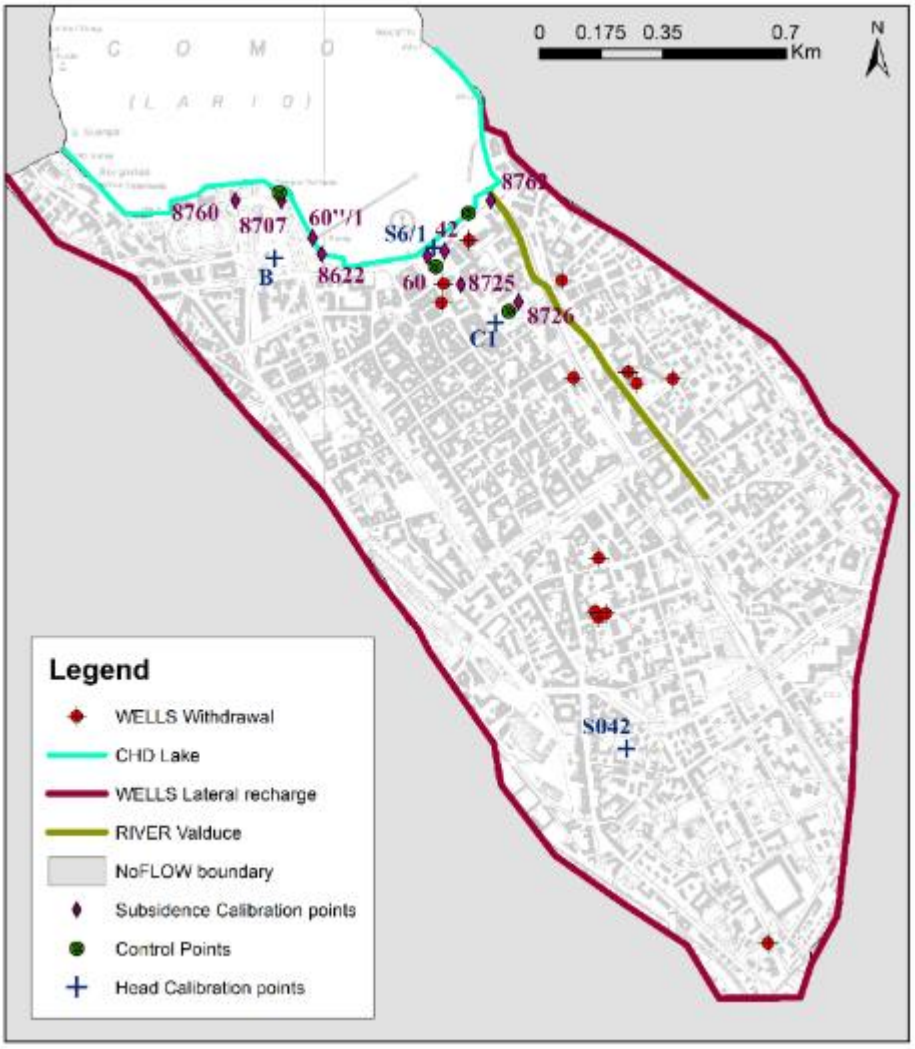

Fig. 7 Model boundary conditions and location of calibration and control points.

fact that in the two years preceding the simulated period the lake level remained on average higher than the ordinary conditions, due to the flooding event of November 2002. The *RIVER* boundary condition was introduced to simulate the influence of the Valduce creek, which has a natural riverbed only in its terminal stretch towards the lake. The *WELLS* condition was used to simulate water withdrawals that reach maximum total values of about 25 l/s (Municipality of Como, 2014), much lower than 150 l/s that, in the past few decades, have caused an acceleration of the subsidence phenomenon (Arca and Beretta, 1985). Wells develop in the first two layers, representing the shallow aquifer, and they are essentially related to industrial or to open loop geothermal enthalpy implants. Runoff deriving from mountainous and forested areas, which border the Como basin, is the primary source of aquifer recharge; in fact, due to the dense urban fabric of the town, the direct recharge was considered negligible. The lateral recharge was estimated of about 450 l/s and was introduced along the entire perimeter of the active zone by means of

fictitious injection wells (*WELLS* lateral recharge). This quantity was obtained by combining the Thornthwaite-Mather Model (Thornthwaite & Mather, 1957) and the Curve Number procedure (SOIL CONSERVATION SERVICE, 1972) on rainfall and temperature data of the surrounding areas. This overall quantity was then subdivided along the perimeter of the model according to the lateral homogeneus areas features (river basin, geological substrate and quaternary deposits, presence of water streams, and land use). Fig. 7 shows the model settings, calibration and control points.

6.3. Hydro-geotechnical parameterization

The aquifer-system initial properties were obtained by the critical analysis of the data collected in the geotechnical and hydrogeological database. Values of selected properties (summarized in Table 2) and stresses were adjusted by *trial and error* technique until satisfying the model calibration phase (Section 6.4).

Unit R texture (pebbles and bricks incorporated in a sandy-silty matrix) is in agreement with its calibrated hydraulic conductivity of 5.3×10^{-4} m/s. Also the value of storage coefficient S = 0.3 assigned to Unit R was derived from pumping tests interpretation; although the primary porosity of sandy-silty soils is rather low, their artificial nature, as well as the remarkable voids (up to 10^{-1} m) detected between the fine matrix and the coarse component, suggest high storage of water in the unit.

Regarding the UGS unit (Layer 2) the results of the on-site permeability tests were analyzed and returned a range of *k* values between 10^{-5} and 10^{-2} m/s. A value of 2.6×10^{-3} m/s was assigned to the unit after the calibration procedure. Due to pumping tests unavailability, an *S* value of 0.2 was given, in accordance with the hydrogeological behavior hypothesized for the shallow aquifer. For layers 3 and 4 (POS and ICS units) only data deriving from the oedometric tests were available. Considering the high presence of the fine sandy component within the POS unit, a *k* value of 7×10^{-6} m/s was given. As for the ICS unit, more compact than the previous one, a *k* value of 4.73×10^{-9} m/s has been assigned. The S values of 0.01 and of 0.006 has been assigned respectively to the third and fourth layer through the analysis of hydrogeological literature combined with calibration procedure.

Parameters related to the compressibility of soils were estimated by oedometric tests, when available, or literature analysis. The values assigned to the different units are presented in Table 2. In particular, UGS unit parameters S_{ske} *and* S_{skv} were set equal to each other to ensure an elastic behavior, typical of granular soils. The same values were assigned to the first Layer sub-unit R_{UC}, which is expected to have a similar behavior to unit UGS. Compressibility parameter values of sub-units R_{LF} and R_C, which are characterized by anthropic deposits, compressibility values were , were derived from the numerous available oedometric tests, mainly carried out during flooding defense works installation. The higher compressibility of sub-unit R_C in comparison to sub-unit R_{LF} is testified by a slightly larger value of S_{skv}.

UNIT	**k(m/s)**	**S(-)**	**S_{ske}(m^{-1})**	**S_{skv}(m^{-1})**
R	$5.3x10^{-4}$	0.3	$6x10^{-6}$	R_c $1.76x10^{-2}$ R_{LF} $1.3x10^{-2}$ R_{UC} $3x10^{-6}$
UGS	$2.6x10^{-3}$	0.2	$3x10^{-6}$	$3x10^{-6}$
POS	$7x10^{-6}$	0.01	$6x10^{-6}$	$4.2x10^{-3}$
ICS	$4.73x10^{-9}$	0.006	$6x10^{-6}$	$3.77x10^{-3}$

Table 2 Input hydro-geotechnical parameters selected for the coupled numerical model.

For the third and fourth layers, a similar procedure was carried out; for both units an elastic value of S_{ske} = $6x10^{-6}$ m^{-1} was chosen based on literature (Hoffman et al., 2003). Due to the presence of organic nature, POS S_{skv} value obtained by oedometric tests, resulted to be slightly higher than the ICS value.

A no delay numerical approach was selected for the compressible units R, POS and ICS. For POS and ICS the choice is justified by their well-defined behavior as aquitards. For R unit the grain-size heterogeneity could suggest the use of the Delay approach. However, from the conceptual model it emerges that the silty-sandy material is not confined to mappable lenses, but rather acts as a matrix to coarser clasts and anthropic artifacts, thus resulting in the more convenient use of No-Delay approach.

6.4. Model Calibration

Groundwater level calibration was based on data recorded at piezometers B, C1, S6/1 and S042 (see location in Fig. 7) in March 2008 and July 2009. With regard to ground deformations, cumulated subsidence measurements recorded between 2004 and 2011 at nine benchmarks

(APAT surveys, cf. Section 3, Fig. 7) were used. The monitoring points are concentrated in the shoreline area; outside the historical town, no critical issues are expected due to the minimum thickness of the R unit and the progressive thinning towards south of the POS unit - the two most compressible units of the succession.

Different indices were calculated to evaluate the model's performance and reliability: maximum error, standard deviation, correlation coefficient and normalized root mean square error (RMS) as reported in Anderson and Woessner (1992). Table 3 reports the values of the performances indices whereas Fig. 8 shows the calculated versus observed values both for head and subsidence.

	Head	**Subsidence**
Maximum error (m)	0.34	0.005
Correlation coefficient	0.98	0.86
Standard Deviation (m)	0.09	0.002
RMS normalized	6.93%	8.53%

Table 3 model quality parameters.

7. Model results and discussion

7.1 Hydrogeological model

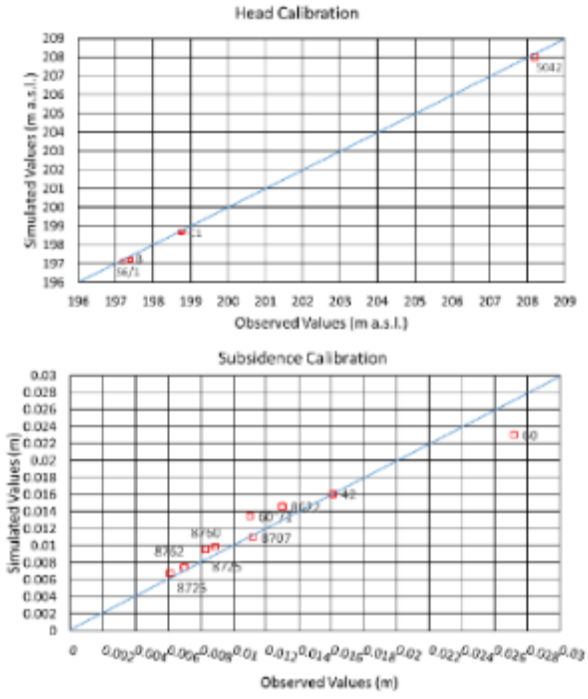

Fig. 8 Head and subsidence (observed vs simulated values) calibration graphs. Location of calibration points is reported in Fig. 2 and Fig. 6.

The simulated surficial aquifer piezometric surface (dashed blue lines in Fig. 9) shows a main direction from SE, at 220 m a.s.l. (in correspondence of the recharge anomaly of the Respaù creek paleo-channel), to NW at 197 m a.s.l. (Lake level). The simulated piezometric surface was evaluated by comparing it to a calculated piezometric surface. The latter was calculated by means of ordinary kriging procedure applied to groundwater levels measured in representative piezometers for the year 2010 and a lake level of 197 m a.s.l. (red lines in Fig. 9).

7.2 Subsidence Model: Lake level dependency

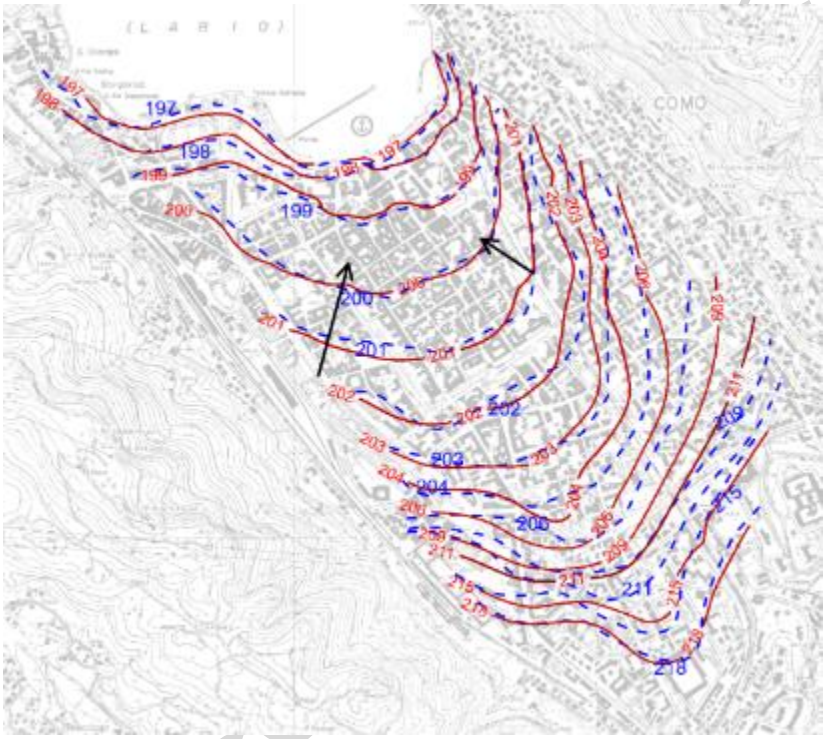

Fig. 9 Simulated (blue dotted lines) and calculated (red lines) piezometric surface for a mean Lake level value of 197 m a.s.l.

In the first phase of the subsidence simulation, the only perturbation introduced was the variation of the average annual height of the lake, as the side recharge have been kept constant throughout the simulated period; the pumping wells, with a total withdrawal of about 25 l/s, were almost irrelevant in the development of the phenomenon. In this way the natural subsidence trend of Como subsoil was investigated. To analyze model response, the same critical areas investigated in the PSInSAR analysis (Section 3.2) were considered and representative results are presented in Fig. 10.

However, the Lungolago Trento area, which is much more affected by the anthropic actions during the simulated period, has to be discussed separately.

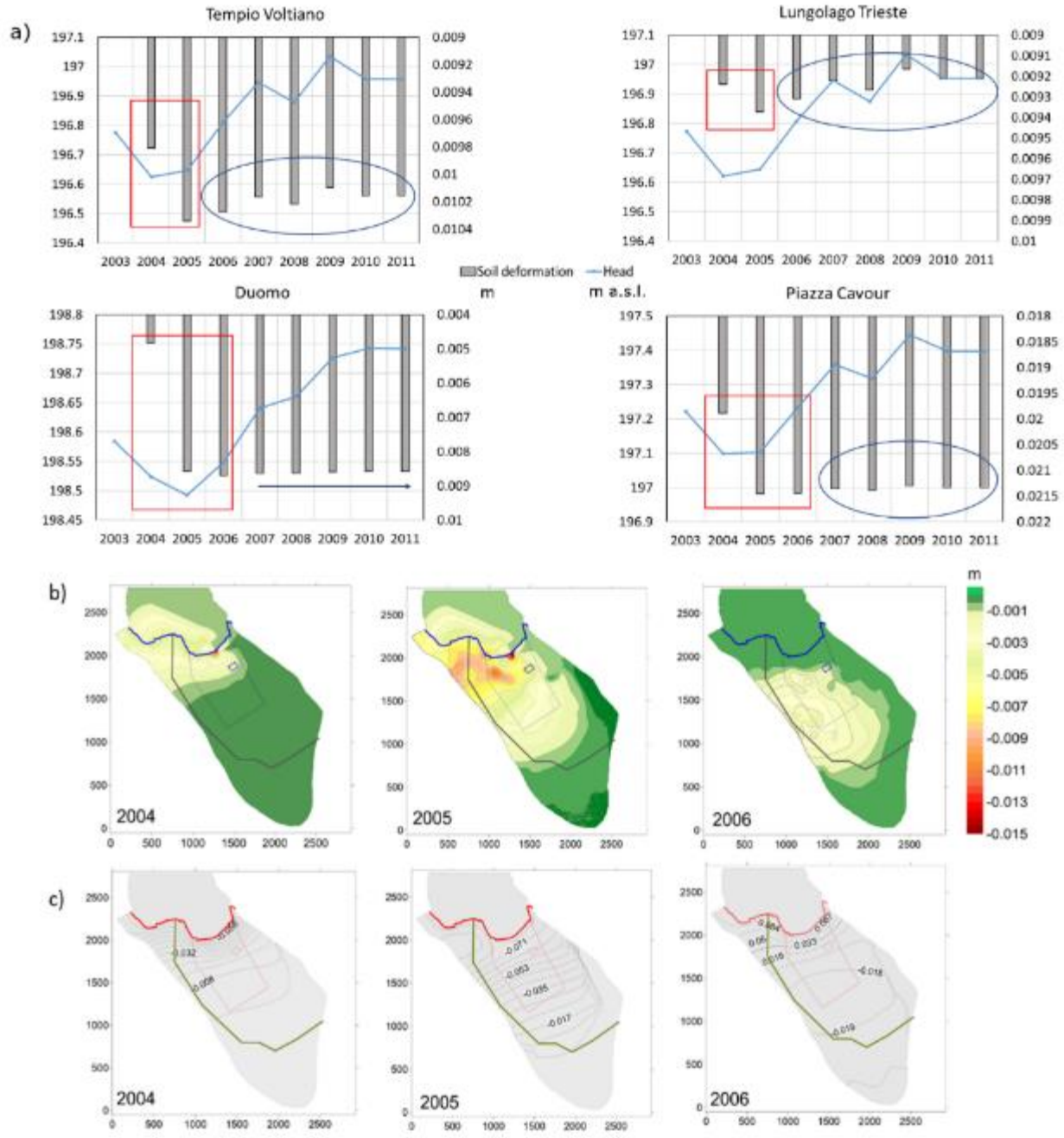

Fig. 10 a) Simulated annual head and cumulate subsidence in the critical areas of the urban area (Check points). Piezometric minima are marked by red polygons and elastic cycles by blue ellipses.The grey arrow indicates a quite stable deformation trend in the Duomo area. b) Simulated annual subsidence variation, in meters c) Simulated annual head variation, in meters. Grey line (b) and green line (c) are a spatial reference for the main street of the city called "Napoleona".

The peak of subsidence is reached essentially between 2004 and 2005, in response to the Lake level and piezometric absolute minimum. The maximum settlement of 2.7 $x10^{-2}$ m is reached in

Cavour Square; the area bordering the west side of the historical town (with 1.6 $x10^{-2}$ m), the area of the Voltiano Temple (with $1x10^{-2}$ m) and the Duomo Square (with 0.87 $x10^{-2}$m) undergoes to a noteworthy deformation, too. These values showed a good agreement with subsidence recorded by high precision levelling benchmark data, as previously seen in model calibration Section 6.4. The southernmost areas of the city record negligible lowering (about 10^{-4}-10^{-5} m globally). After 2005, the lake level varied with a rises and drops trend, causing in an equivalent oscillation of groundwater level. Piezometric head changes are particularly evident along the shoreline, while Duomo area does not present any significant variation (Fig. 10a). These oscillations remained above the piezometric minima recorded during the 2004-2005 period (red polygons in Fig. 10a), inducing only elastic compaction and swelling cycles of the order of 10^{-4}-10^{-5} m (blue ellipses in Fig. 10a). Therefore, the 2004-2005 piezometric minima represented the equivalent reference of the natural pre-consolidation stress of the simulated period. Piezometric lowering, up to a maximum of $4x10^{-2}$ m, were also recorded at the west side of the historical town during 2006. In this area, the shallower layer is constituted by the sub-unit RUC, which shows very low compressibility. Therefore, the simulated compaction is due to the POS unit, which reaches its maximum thickness there. In general, most of the deformation occurred from 2004 to 2006 (i.e. Fig. 10b-c) while no significant variations, linked to natural perturbations, are recorded by the model until the end of the simulated period.

7.3 Subsidence Model: additional anthropic perturbation

During 2008 and 2009, due to the installation of the Pool B, a groundwater pumping of 115 l/s was

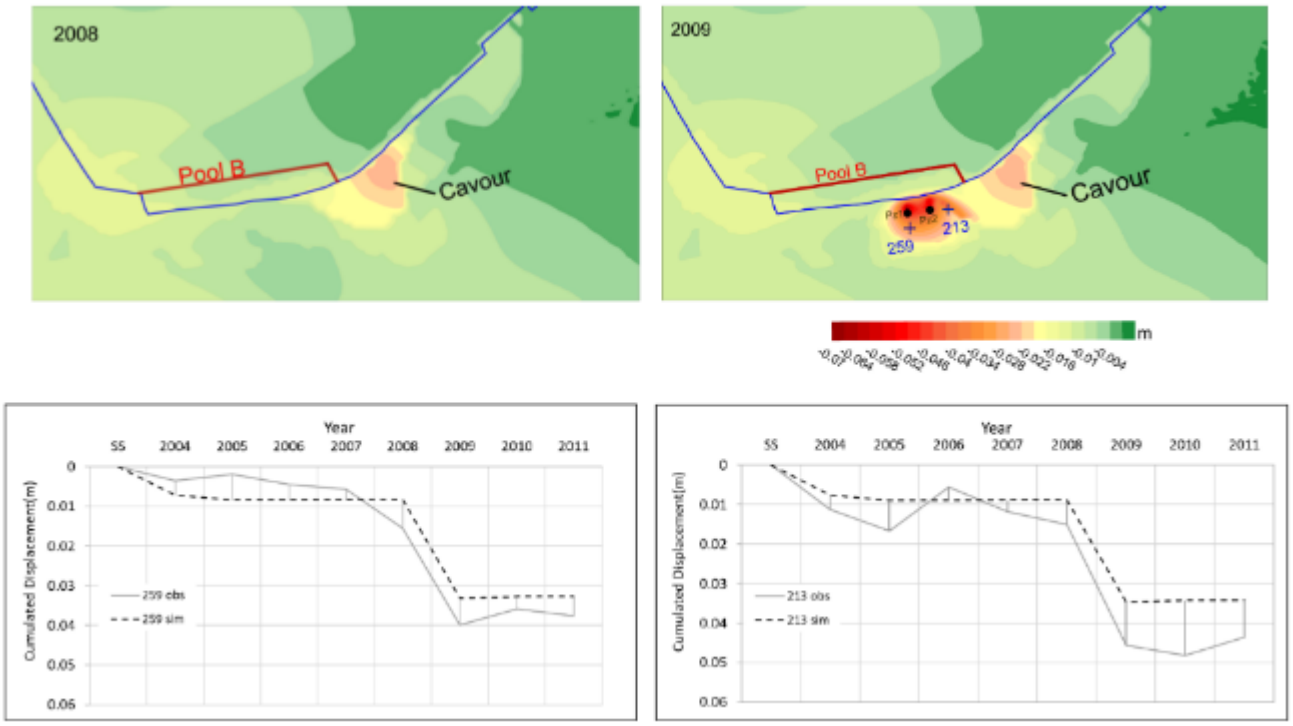

Fig. 11 Local subsidence maximum developed in 2009 and located in the construction site of pool B, in the Lungolago Trento area. A comparison between subsidence previous wells installation (2008) is provided. The two plots show observed (continue grey line) and simulated (dotted black line) cumulated subsidence in the verification points.

operated in the *Lungolago Trento* area by means of two pumping wells (E.G., 2011). This localized anthropic perturbation was thus introduced in the model and was validated by PZ1 and PZ2 piezometers and to the satellite Permanent Scatters n° 213 and 259, located in the proximity of the pumping wells. This scenario allowed both to verify the model and to analyze the acceleration of natural subsidence phenomenon by means of groundwater withdrawal/exploitation. Natural induced subsidence simulated along Lungolago Trento was about 1-1.5 meters. The induced groundwater drop of 2-2.5 m caused a very localized (only reaching the western part of *Piazza Cavour*) and almost instantaneous acceleration in soil compaction in the area of the construction site (Fig. 11).

From groundwater level analysis, it emerged that the natural groundwater regime was essentially reestablished and recovered in 2010, when the pumping in the construction site ceased. The simulation reports a consistent subsidence between 6-7 $x10^{-2}$ m in correspondence with the pumping wells, which decreases with increasing distance from the capture zone (about 3-4 $x10^{-2}$ m

recorded in PS n° 213 and 259) and was not recovered after 2009. Soil behavior simulated by model and PS showed an almost instantaneous response to the perturbation but they differ slightly in term of absolute values. As previously explained in Section 3.2, since no high precision benchmarks were available in the *Lungolago Trento* area for the period 2004-2011, only PS data could be used to validate this model step. This scenario suggests that the units identified in the urban area have not reached the maximum degree of consolidation yet. Therefore, soils could experience significant further lowering in case of external perturbations (natural or artificial) able to drop groundwater levels consistently below the recorded minimum of 2004-2005, thus representing a new value of pre-consolidation stress for the study area.

Due to the different resolution and temporal acquisition scale, a comparison between satellite and numerical simulation absolute values of displacement time series is unfeasible. Satellite data show very low (few millimeters) displacements seasonal oscillations, that are not recorded by the numerical model. However, the aim of the latter is to allow a general understanding and quantification of the phenomenon in a forecasting and urban management perspective. Therefore, a perfect simulation of low seasonal oscillations is out of scope. Despite these discrepancies, model (Fig. 12a) and processed PSInSAR (Fig. 12b) cumulated subsidence values are in good agreement, especially in term of recognition of the most critical areas (Fig. 12c).

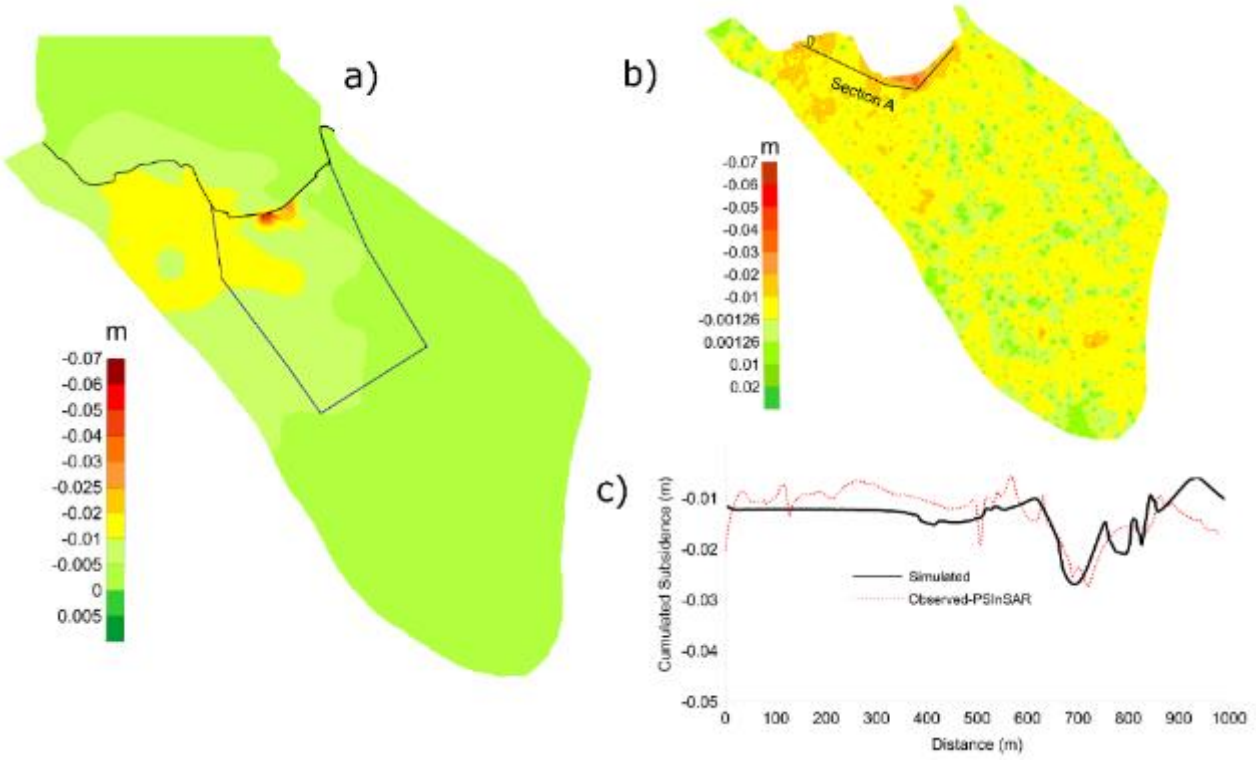

Fig. 12 a) Simulated cumulated subsidence in 2011. b) Cumulated subsidence in 2011 derived from interpolation and processing of Permanent scatters time series. c) Cumulated observed and simulated subsidence along section A.

To explain the dependency between geological, geotechnical, hydrogeological features and the Como subsidence simulated results, an analytical analysis of soil nature, soil thickness, and soil deformation was carried out. The soil deformation versus time graphs, in relation with the unit thickness (Fig. 13), show that the R (sub-units R_C and R_{LF}) and POS units, in accordance with their

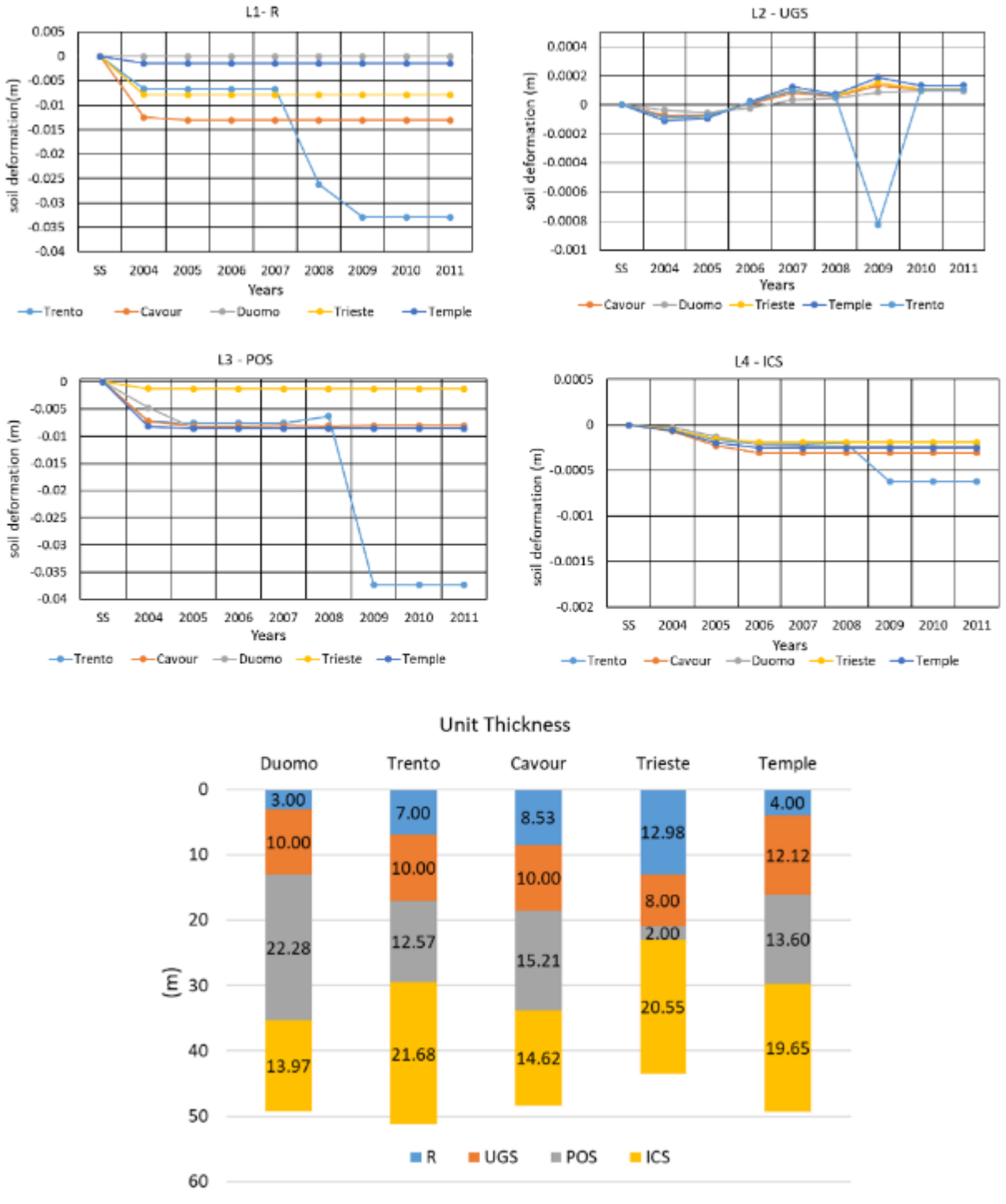

Fig. 13 Annual soil deformation by unit (note the vertical exaggeration for ICS and UGS units) and unit thickness calculated in the control points.

high compressibility nature, contributed almost to the entire deformation recorded in the study area.

The ICS unit contribution to the global subsidence phenomenon is negligible. Due to its high depth and low hydraulic conductivity, the hydraulic and the effective stress variations were mainly adsorbed by the shallower units. The elastic recovery of the deformation, even if in marginal terms with respect to the whole phenomenon, is to be attribute to the UGS unit, in accordance with the geotechnical nature of the soils constituting it. The anomalous soil deformation behavior simulated in the Lungolago Trento area is coherent with the groundwater pumping activities undergone during the 2008-2009 defense works.

The use of *no-delay beds*, leads to an almost instantaneous deformation response to the variation of the hydraulic head. This means that the time evolution of subsidence on site could be delayed in comparison to the piezometric oscillations and the modelled process, despite the absolute value of cumulated displacement is coherent. Thus, the subsidence trend has to be considered more

UNIT	**Sskv (m-1)**	**bav (m)**	**Kv (m/s)**	**τ**
R	1.3x10-2	8	5.3x10-5	Instantaneous (<1day)
POS	4.2x10-3	30	7x10-7	2.5 years
ICS	3.77x10-3	40	4.73x10-9	>10 years

UNIT	**S_{skv} (m^{-1})**	**b_{av} (m)**	**K_v (m/s)**	**τ**
R	$1.3x10^{-2}$	8	$5.3x10^{-5}$	Instantaneous (<1day)
POS	$4.2x10^{-3}$	30	$7x10^{-7}$	2.5 years
ICS	$3.77x10^{-3}$	40	$4.73x10^{-9}$	>10 years

gradual in term of time evolution, as shown by satellite data.

Table 4 *shows* an attempt to estimate the not simulated delay time τ (because of the implemented *No-delay* beds approach) of each compressible unit by equation (4).

Table 4 Estimating time delay of cohesive units by Riley equation.

The deformation results almost instantaneous for unit R, due to its high compressibility and k value. Conversely, the completion of the deformation of unit ICS exceeds the simulation time,

assessing that the completion of the process is more gradual. Data in Table 4 indicates that delays in areas where R thickness is lower than both POS and ICS units are very likely.

8. CONCLUSIONS

Any natural or anthropogenic perturbation of the groundwater level can induce a deformation of the solid skeleton of soils constituting the aquifer system. Through the case study of the Como historical urban area, an effective numerical model for the assessment of the phenomenon of subsidence was built. The calibrated and evaluated model can be used as a support in groundwater management.

To develop a critical analysis of the phenomenon, a geotechnical and hydrogeological dataset was created, including information dating back to the 70s. The database was used as source for the development of the conceptual model of the subsoil and for the parameterization of the numerical model of flow and subsidence. The environmental conditions potentially able to trigger land subsidence are, in the absence of anthropic disturbances, the variation of the piezometric regime in the shallow and deep confined aquifers, and fluctuations of the lake level.

The numerical model presents some limitations and assumptions. First, the most complete and recent monitoring data refer to the period 2004-2011. After this date, lake flooding defenses have been installed, which may have consistently varied the relationship between the Lake and groundwater. Availability of more recent geotechnical and piezometric monitoring data would allow including such modifications of the shoreline structure, to update and extend model simulations to the current days.. Secondly, the recharge value of the aquifer has been kept constant for the entire simulation period. Although in the simulated period no exceptional precipitation, deviating from the assumed average values, was recorded, a more differentiated quantification of the atmospheric input might be considered.

Model simulations pointed out the critical nature of the superficial reworked anthropogenic materials in governing the subsidence phenomenon. In particular, the model could be used, as for the B pool, to evaluate any deformation related to the construction of the A pool (not yet completed) located in the *Lungolago Trieste,* where the unit R thickness is consistent (12 m).

Therefore, a local lake front scale model, with a very accurate stratigraphic discretization of this

unit (not possible at the basin scale), could represent a useful tool for the groundwater management of the urban area.

The developed numerical model represents a valuable tool to forecast future subsidence scenarios, with respect to natural or anthropic perturbation of groundwater level in term of spatial evolution. High precision leveling and satellite monitoring data are necessary tools for identifying trend variations and discrepancies from the numerical simulation previsions, and thus for planning the most resolutive actions. Modelling and monitoring approaches should be combined to reach a comprehensive spatial and temporal prevision of the subsidence phenomenon.

Acknowledgments

The authors would like to thank the Como Municipality and E.G. Engineering Geology for data supplying. Thanks to Dr. J. Terrenghi for the support in the numerical modelling and Dr. C. Camera for the useful suggestions. The authors acknowledge the two anonymous reviewers for their high-quality suggestions, which improved the quality of the paper.

Funding

This research did not receive any specific grant from funding agencies in the public, commercial, or not-for-profit sectors.

Declarations of interest: none

REFERENCES

ANDERSON M.P., WOESSNER W.W. (1992): Applied groundwater modeling. Academic Press, San Diego, CA.,381 pp.

ANTONIELLI, B., MONSERRAT, O., BONINI, M., CENNI, N., DEVANTHÉRY, N., RIGHINI, G., SANI, F. (2016): Persistent Scatterer Interferometry analysis of ground deformation in the Po Plain (Piacenza-Reggio Emilia sector, Northern Italy): seismo-tectonic implications. Geophysical Journal International 206, 1440–1455. https://doi.org/10.1093/gji/ggw227

APUANI T., CANCELLI A. & CANCELLI P. (2000): Hydrogeological and geotechnical investigations along the shoreline of the town of Como, Italy. In: D.P. Moore & O. Hungr (Eds.) “Engineering Geology and Environment” Proc. 8th. Cong. Intern. Assoc. Engineering Geology (IAEG).

ARCA S. & BERETTA G. P. (1985): Prima sintesi geodetico-geologica sui movimenti verticali del suolo nell’Italia Settentrionale (1897-1957). [First geodetic-geological synthesis on soil vertical movements in Northern Italy (1897-1957)]. Bollettino di Geodesia e Scienze Affini, XLIV, n. 2, pp.125-156.

BARZAGHI R., PASSONI L., PINTO L. & SANSÒ F. (2011): Livellazione di alta precisione e misurazione di rete GNSS di controllo per l’analisi della subsidenza della sponda meridionale del lago di Como, Rapporto tecnico, 37 pp. [High precision leveling and measurement of GNSS control network for the analysis of subsidence in the southern shore of Lake Como ,Technical Report.]

BONCI L., CAMETTI A., COMERCI V., MATARAZZO D., MICHETTI A. M., VITTORI E. & VULLO F. (2004): Città di Como - Livellazione di Alta Precisione (APAT-Dipartimento di difesa del suolo). Rapporto tecnico [Como city – high precision levelling. (APAT – Soil defence department). Technical report].

CARBOGNIN L., TEATINI P., TOSI L. (2004): Eustasy and land subsidence in the Venice Lagoon at the beginning of the new millennium. Journal of Marine Systems, 51(1-4), 345-353 https://doi.org/10.1016/j.jmarsys.2004.05.021

CIAMPALINI, A., BARDI, F., BIANCHINI, S., FRODELLA, W., VENTISETTE, C.D., MORETTI, S., CASAGLI, N. (2014): Analysis of building deformation in landslide area using multisensor PSInSAR™ technique. International Journal of Applied Earth Observation and Geoinformation 33, 166–180. https://doi.org/https://doi.org/10.1016/j.jag.2014.05.011

COMERCI V., CAPELLETTI S., MICHETTI A.M., ROSSI S., SERVA L. & VITTORI E. (2007): Land subsidence and Late Glacial environmental evolution of the Como urban area (Northern Italy). Quaternary International, 173–174, pp. 67-86. https://doi.org/10.1016/j.quaint.2007.06.014

D'APOLLONIA, E. (1970): Dynamic loadings. Journal of the Soil Mechanics and Foundations Division, ASCE, Vol. 96, Issue 1, pp. 49-72.

E.G. ENGINEERING GEOLOGY (2011): Opere di difesa dalle esondazioni del Lago nel comparto Piazza Cavour – Lungolago di Como. Analisi degli effetti indotti sulla falda superficiale nella fase di realizzazione della "Vasca A" Lungo Lario Trieste. Pp.53. Rapporto tecnico. [Defense works against Lake flooding in the Piazza Cavour - Como lake area. Analysis of the effects induced on the surficial water table during the realization of the "pool A" in Lungolario Trieste.Technical Report.]

FERRARIO, M.F., BONADEO, L., BRUNAMONTE, F., LIVIO, F., MARTINELLI, E., MICHETTI, A.M., NERI, P.C., CHIESSI, V., COMERCI, V., HÖBIG, N., (2015): Late Quaternary environmental evolution of the Como urban area (Northern Italy): A multidisciplinary tool for risk management and urban planning. Engineering Geology 193, 384–401. https://doi.org/10.1016/j.enggeo.2015.05.013

FERRETTI, A., PRATI, C., ROCCA, F., (2000): Nonlinear subsidence rate estimation usingpermanent scatterers in differential SAR interferometry. IEEE Trans. Geosci. Rem.Sens. 38, 2202–2212.

GALLOWAY, D.L., BURBEY, T.J. (2011): Review: Regional land subsidence accompanying groundwater extraction. Hydrogeology Journal 19, 1459–1486. https://doi.org/10.1007/s10040-011-0775-5

GALLOWAY, D.L., HOFFMANN, J., & ZEBKER, H.A. (2003): Inverse modeling of interbed storage parameters using land subsidence observations, Antelope Valley, California. Water Resources Research 39.

GU, K., SHI, B., LIU, C., JIANG, H., LI, T., WU, J., (2018): Investigation of land subsidence with the combination of distributed fiber optic sensing techniques and microstructure analysis of soils. Engineering Geology 240, 34–47. https://doi.org/https://doi.org/10.1016/j.enggeo.2018.04.004

HARBAUGH A.W, BANTA E.R., HILL M.C. & MCDONALD M.G. (2000): MODFLOW-2000, the U.S. geological survey modular groundwater model - user guide to modularization concepts and the groundwater flow process. Open-file report 00-92. Pp. 54.

HERRERA, G., TOMÁS, R., MONELLS, D., CENTOLANZA, G., MALLORQUÍ, J.J., VICENTE, F., NAVARRO, V.D., LOPEZ-SANCHEZ, J.M., SANABRIA, M., CANO, M., MULAS, J. (2010): Analysis of subsidence using TerraSAR-X data: Murcia case study. Engineering Geology 116, 284–295. https://doi.org/10.1016/j.enggeo.2010.09.010

HOFFMANN J., LEAKE S.A., GALLOWAY D.L. & WILSON A.M. (2003): MODFLOW-2000 Ground-water model user guide to the subsidence and aquifer-system compaction (sub) package. USGS Open-File Report 03-233.

IVY-OCHS, S., KERSCHNER, H., MAISCH, M., CHRISTL, M., KUBIK, P. W., & SCHLÜCHTER, C. (2009): Latest Pleistocene and Holocene glacier variations in the European Alps. Quaternary Science Reviews, 28(21-22), 2137-2149. https://doi.org/10.1016/j.quascirev.2009.03.009

MAHMOUDPOUR, M., KHAMEHCHIYAN, M., NIKUDEL, M.R., & GHASSEMI, M.R. (2016): Numerical simulation and prediction of regional land subsidence caused by groundwater exploitation in the southwest plain of Tehran, Iran. Engineering Geology 201, pp. 6–28. https://doi.org/10.1016/j.enggeo.2015.12.004

MECKEL, T.A., TEN BRINK, U.S., & WILLIAMS, S.J. (2006): Current subsidence rates due to compaction of Holocene sediments in southern Louisiana. Geophysical Research Letters 33. doi: 10.1029/2006GL026300

MENZENBACH E. (1959): Die Anwendbarkeit von Sonden zur Prüfung der Festigkeitseigenschaften des Baugrundes. Forschungsberichte des Landes Nordrhein-Westfalen, n. 713 [The applicability of probes for testing the strength properties of the subsoil. Research Reports of the State of North Rhine-Westphalia, n. 713]

MICHETTI A.M., LIVIO F., PASQUARÉ F.A., VEZZOLI L., BINI A., BERNOULLI D., SCIUNNACH D. - SERVIZIO GEOLOGICO D'ITALIA (2013): Carta Geologica d'Italia a scala 1:50.000, Progetto CARG Foglio 075 – Como. ISPRA – Dipartimento Difesa del Suolo. Note Illustrative del Foglio 075 – Como. 206 pp.[CARG Project , Sheet 075 – Como. Geological Map of Italy, illustrative notes.]

MUNICIPALITY OF COMO (2014): Opere per la difesa dalle esondazioni del Lago nel comparto Piazza Cavour - Lungo Lago di Como, Rapporto Tecnico, Pp. 216. [Defense works against Lake flooding in Piazza Cavour – Como lakefront area, Technical report]

PACHECO-MARTÍNEZ, J., HERNANDEZ-MARÍN, M., BURBEY, T.J., GONZÁLEZ-CERVANTES, N., ORTÍZ-LOZANO, J.Á., ZERMEÑO-DE-LEON, M.E., SOLÍS-PINTO, A., (2013): Land subsidence and ground failure associated to groundwater exploitation in the Aguascalientes Valley, México. Engineering Geology 164, 172–186. https://doi.org/https://doi.org/10.1016/j.enggeo.2013.06.015

PHIEN-WEJ, N., GIAO, P.H., NUTALAYA, P., (2006): Land subsidence in Bangkok, Thailand. Engineering Geology 82, 187–201. https://doi.org/https://doi.org/10.1016/j.enggeo.2005.10.004

RILEY FS (1969): Analysis of borehole extensometer data from central California. Land subsidence. Int Assoc Sci Hydrol Publ 89(2), pp. 423–431

SANGLERAT G. (1972): The penetration and soil exploration. Development in geotechnical engineering, Elsevier Sci-entific Publishing, New York, pp. 52-80.

SCHMERTMANN J.H., HARTMAN J.P. & BROWN P.R. (1978): Improved strain influence factor diagrams. Journal of the Geotechnical Engineering Division, 104(GT8), pp. 1131-1135.

SHI, X., FANG, R., WU, J., XU, H., SUN, Y., YU, J., (2012): Sustainable development and utilization of groundwater resources considering land subsidence in Suzhou, China. Engineering Geology 124, 77–89. https://doi.org/https://doi.org/10.1016/j.enggeo.2011.10.005

SHI, X., WU, J., YE, S., ZHANG, Y., XUE, Y., WEI, Z., LI, Q., YU, J. (2008): Regional land subsidence simulation in Su-Xi-Chang area and Shanghai City, China. Engineering Geology 100, 27–42. https://doi.org/10.1016/j.enggeo.2008.02.011

SNEED, M. (2001): Hydraulic & mechanical properties affecting ground-water flow & aquifer-system compaction, San Joaquin Valley, California. USGS Open file Report 35-26.

SOIL CONSERVATION SERVICE (1972): National Engineering Handbook, section 4, Hydrology, U.S. Department of Agriculture, Washington D.C., U.S.A.

SOWERS G.B. (1970): Introductory Soil Mechanics and Foundations, The Macmillan Company, Collier Macmillan Limited, London, 3rd Edition, 102 pp.

TERZAGHI, K. (1925): Principles of soil mechanics: IV; Settlement and consolidation of clay. Erdbaummechanic 95 (3), 874–878.

THOANG, T.T., GIAO, P.H., (2015): Subsurface characterization and prediction of land subsidence for HCM City, Vietnam. Engineering Geology 199, 107–124.
https://doi.org/https://doi.org/10.1016/j.enggeo.2015.10.009

THORNTHWAITE, C.W. & MATHER J.R. (1957): Instructions and tables for computing potential evapotranspiration and the water balance: Centeron, N.J., Laboratory of Climatology, Publications in Climatology, 10 (3), pp. 185-311.

TRE - Telerilevamento Europa (2012): Rapporto tecnico [Technical report], p. 66.

WOOD, D. M. (1990): Soil behaviour and critical state soil mechanics Cambridge University Press, Cambridge, UK

ZHANG, Y., XUE, Y.-Q., WU, J.-C., YE, S.-J., WEI, Z.-X., LI, Q.-F., YU, J. (2007): Characteristics of aquifer system deformation in the Southern Yangtse Delta, China. Engineering Geology 90, 160–173. https://doi.org/10.1016/j.enggeo.2007.01.004

ZHU, L., GONG, H., LI, X., WANG, R., CHEN, B., DAI, Z., TEATINI, P., (2015): Land subsidence due to groundwater withdrawal in the northern Beijing plain, China. Engineering Geology 193, 243–255. https://doi.org/https://doi.org/10.1016/j.enggeo.2015.04.020

HIGHLIGHTS

- A coupled hydro-geotechnical numerical model for Como urban area was developed.
- Numerical model was integrated with satellite and levelling monitoring data.
- Reworked anthropic soils are critical in governing subsidence along the shoreline.
- Anthropic perturbations of groundwater flow enhance subsidence up to 6-7 cm per year.
- Future completion of Lake's floods defense system could develop new critical areas.